Supporting Information

Charged Poly(N-isopropylacrylamide) Nanogels for Use as Differential Protein Receptors in a Turbidimetric Sensor Array

Heidi R. Culver[a,b], Ishna Sharma[c], Marissa E. Wechsler[a,b], Eric V. Anslyn[d], Nicholas A. Peppas[a,b,e,f,g,*]

[a]Institute for Biomaterials, Drug Delivery, and Regenerative Medicine, [b]Department of Biomedical Engineering, [c]Department of Electrical and Computer Engineering, [d]Department of Chemistry, [e]McKetta Department of Chemical Engineering, [f]College of Pharmacy, and [g]Department of Pediatrics, Dell Medical School, The University of Texas at Austin, Austin, TX, 78712, United States

Table of contents:

Experimental methods

Materials

Poly(ethylene glycol) methacrylate (PEGMA) (MW of PEG block = 400) was purchased from Polysciences, Inc. (Warrington, PA). Pure agmatine sulfate powder from BulkSupplements.com was purchased through Amazon.com. 10X PBS, Tris Base, 1-Ethyl-3-(3-dimethylaminopropyl)carbodiimide) (EDC), and ethylenediamine dihydrochloride were purchased from Thermo Fisher Scientific (Waltham, MA). Ultrapure water (final resistance = 18.2 MΩ) was obtained from a Barnstead GenPure purification system from Thermo Fisher Scientific. Spectra/Por dialysis tubing was used for dialysis (12-14 kDa MWCO). Lysozyme from chicken egg white, trypsin from bovine pancreas, cytochrome c from bovine heart, lactoferrin from human milk, hemoglobin from bovine blood, myoglobin from equine skeletal muscle, gamma globulins from bovine blood, bovine serum albumin, ovomucoid from chicken egg white (i.e., trypsin inhibitor type II-O), fetuin from bovine blood, ovalbumin, and all other reagents were purchased from Sigma-Aldrich (St. Louis, MO).

Poly(NIPAM-co-MAA) nanogel synthesis

Poly(NIPAM-co-MAA) nanogels were synthesized via precipitation polymerization in water. N-isopropylacrylamide (NIPAM) and methacrylic acid (MAA) were combined in ultrapure water at a molar ratio of 4:1 for a final monomer concentration of 15 mM. N,N'-methylenebisacrylamide (BIS) was added at 15% relative to monomer. The monomer solution was nitrogen purged while heating to 70°C for 40 minutes and then polymerization was initiated with a freshly prepared solution of ammonium persulfate (APS) for a final initiator concentration of 0.88 mM. Polymerization was carried out at 70°C for 4h after which nanogels were cooled and dialyzed against ultrapure water at room temperature for 4-5 days with 3 water changes in the first 24 hours and ~1 water change every 12 hours for the until the water had been changed 8-10 times. Nanogels were lyophilized and stored at room temperature until further use. Synthesis was repeated in triplicate. Poly(NIPAM-co-MAA) nanogels were dissolved at 0.125 mg/mL in 5 mM KCl and titrated with 0.01N NaOH to estimate the moles of carboxylic acid per milligram of nanogels.

Nanogel modification

Lyophilized nanogels were suspended at 5 mg/mL in 50 mM MES (pH 6.0) coupling buffer. The ligand being coupled (i.e., 2-aminoethyl hydrogen sulfate (AEHS), agmatine sulfate (AGS), N-methylethylenediamine (NMEDA), or ethylenediamine dihydrochloride (ED)) was dissolved in the coupling buffer at 8-times molar excess relative to the number of carboxylic acid groups and titrated to pH 6.0 with 1N HCl when necessary. Nanogels, amine, and freshly prepared EDC (25 mg/mL) solutions were combined in a 10:5:1 volume ratio. The reaction was carried out for 4h at room temperature while mixing end-over-end. To improve the coupling efficiency of AGS, guanidinium hydrochloride was included at an equal molar ratio to AGS. Subsequently the reaction was quenched with an equal volume of 100 mM Tris (pH 10.0). The modified nanogels were dialyzed against ultrapure water at room temperature for 4-5 days with 3 water changes in the first 24 hours and ~1 water change every 12 hours for the until the water had been changed 8-10 times. Modified nanogels were lyophilized and stored at room temperature until further use.

Characterization of modified nanogels

Poly(NIPAM-co-MAA) nanogels were characterized before and after modification with each ligand. For characterization by dynamic light scattering (Malvern ZetaSizer Nano-ZS), lyophilized nanogels were re-suspended in 0.1X phosphate buffered saline (PBS, pH 7.4: 10 mM Na_2HPO_4, 1.8 mM KH_2PO_4, 13.7 mM NaCl, 0.27 mM KCl; ionic strength =17.3 mM) or 0.1X histidine buffered saline (HBS, pH 5.5: 2.5 mM L-histidine, 14 mM NaCl; ionic strength = 17.4 mM) at 1 mg/mL, probe sonicated, and titrated to pH 7.4 ± 0.1 or 5.5 ± 0.1, respectively. For characterization by transmission electron microscopy (FEI Tecnai TEM operating at 80 kV), lyophilized nanogels were re-suspended in ultrapure water at 0.5 mg/mL and probe-sonicated. Nanogels on ionized carbon coated 400 mesh copper grids were stained with 2% uranyl acetate. For titration (Hanna Instruments 902 Potentiometric Titrator), nanogels (5 mg) were dissolved in 5 mM KCl at 0.125 mg/mL and the initial pH was adjusted to approximately 3.8 by the addition of 1N HCl (10μL). Based on a literature pK_a value for MAA of 4.65, it was assumed that 88% of the carboxylic acid groups were deprotonated at the initial pH (~3.8). The particles were titrated with 0.01N NaOH to pH 10.0. The number of moles of carboxyl group per mass of nanogel (n_{COOH}/mg nanogel) was calculated using **Equation 1**:

$$n_{COOH}/\text{mg nanogel} = 0.88(N_{NaOH}V_{NaOH} - n_{HCl})/5 \text{ mg nanogel} \quad (1)$$

where N_{NaOH} is the normality of the base added (0.01N = 10 μmol/mL), V_{NaOH} is the volume of base added to reach the equivalence point (mL) and n_{HCl} is the number of moles of HCl added (10 μmol). The efficiency of modification was then calculated as the difference between micromoles of carboxyl groups before and after carbodiimide coupling. Additionally, specific incorporation of the functional groups was confirmed by FTIR (Thermo Fisher Scientific) and ^{1}H NMR spectroscopy (Varian DirectDrive, 600 MHz). For ^{1}H NMR, polymers were dissolved at a concentration of at least 10 mg/mL in D_2O.

Protein binding studies

Buffer conditions for protein binding were optimized using lysozyme and **R1** nanogels. Nanogels were suspended at 0.6 mg/mL in 0.1X PBS (pH 7.4) or 1X PBS (pH 7.4), with or without 0.05% tween 20, and at room temperature or 37°C. Results suggested optimal protein binding in lower ionic strength buffer with no effect of temperature or tween 20. Thus, the remainder of the studies were performed in 0.1X PBS (pH 7.4) or 0.1X HBS (pH 5.5). Specifically, modified and unmodified nanogels were suspended at 0.6 mg/mL in 0.1X PBS (pH 7.4) or 0.1X HBS (pH 5.5) and titrated to the appropriate pH ± 0.1 with 1N HCl or 1N NaOH as needed. Proteins were dissolved in the same buffer (1 mg/mL) and combined in a 1:1 volume ratio with the nanogel solutions. Nanogels and proteins were allowed to incubate together for 1h at room temperature with gentle mixing. As a control, nanogels were

incubated with buffer in the absence of protein. After 1h, particles and any bound protein were centrifuged (21,800*g*, 15 min) and the concentration of protein that had not bound to the particles was determined by a MicroBCA assay (ThermoFisher). The assay was performed according to manufacturer's instructions. The adsorption capacity (Q) was calculated using **Equation 2**:

$$Q = (C_0 - C_e)V/m \qquad (2)$$

where C_o and C_e are the initial and equilibrium protein concentrations (mg/mL), respectively, V is the binding volume (mL), and m is the mass of nanogels used (mg).

For turbidity studies, the nanogels and protein solutions (final concentration of each: 0.5 mg/mL) were prepared as described above and combined in an equal volume in a 96 well plate and allowed to incubate for 1 hour. For the simulated tear study, the concentration of lysozyme was varied from 0 – 0.2 mg/mL while keeping the concentrations of all other tear components constant (**Table S2**). The absorbance at 675 nm was measured using a Cytation 3 Cell Imaging Multi-Mode Plate Reader (BioTek Instruments). Turbidity (τ) was calculated using **Equation 3**:

$$\tau = -(1/L)\ln(T) \qquad (3)$$

where L is the pathlength and T is the transmittance. The relative turbidity ($\tau_{protein}/\tau_{buffer}$) was used as input for multivariate analysis. Data collected from these studies were analyzed using principal component analysis (PCA) and linear discriminant analysis (LDA) in RStudio version 0.99.903.

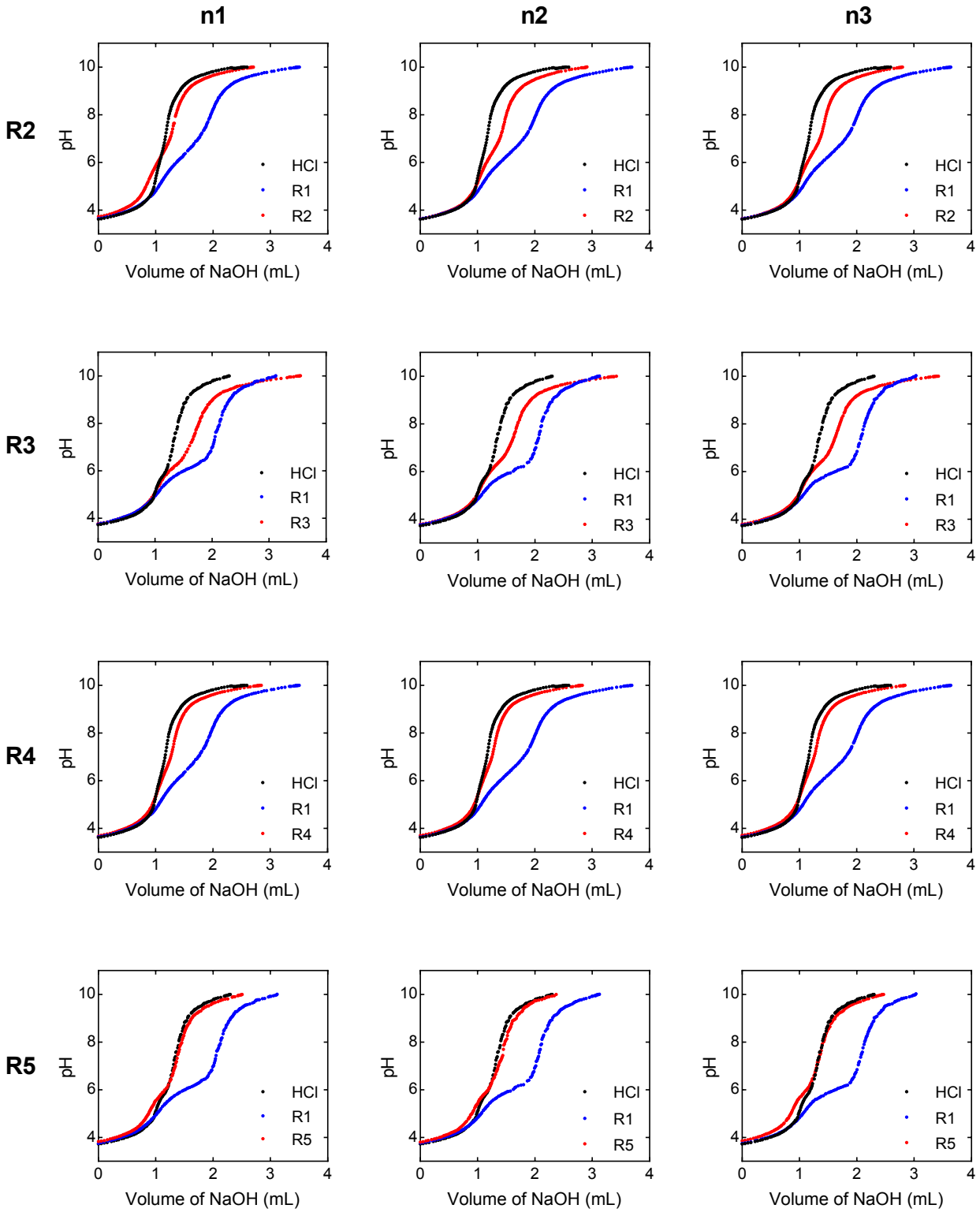

Figure S1. Potentiometric titration of modified poly(NIPAM-co-MAA) nanogels. Lyophilized poly(NIPAM-co-MAA) nanogels (before and after modification) were dissolved at 0.125 mg/mL in 5 mM KCl and titrated with 0.01N NaOH to estimate the moles of carboxylic acid per milligram of NPs.

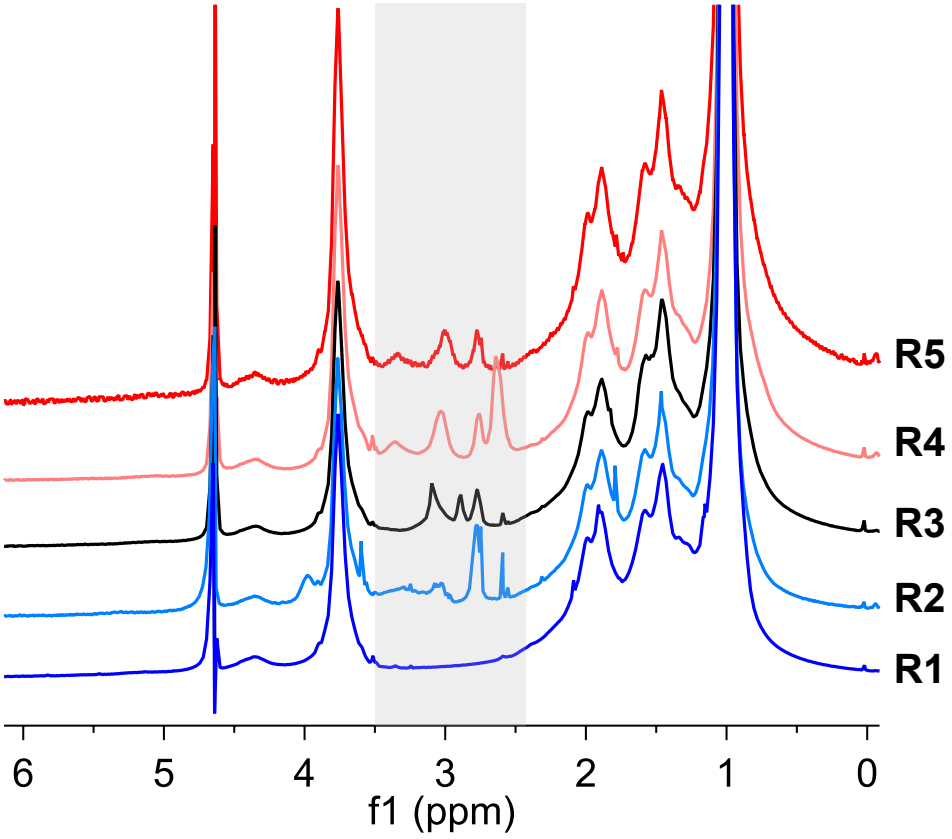

Figure S2. ^{1}H NMR spectra of modified poly(NIPAM-co-MAA) nanogels. ^{1}H NMR (600 MHz, D_2O) Peaks that appeared between δ3.5 – δ2.5 ppm correspond to methyl/methylene protons of the amine ligands.

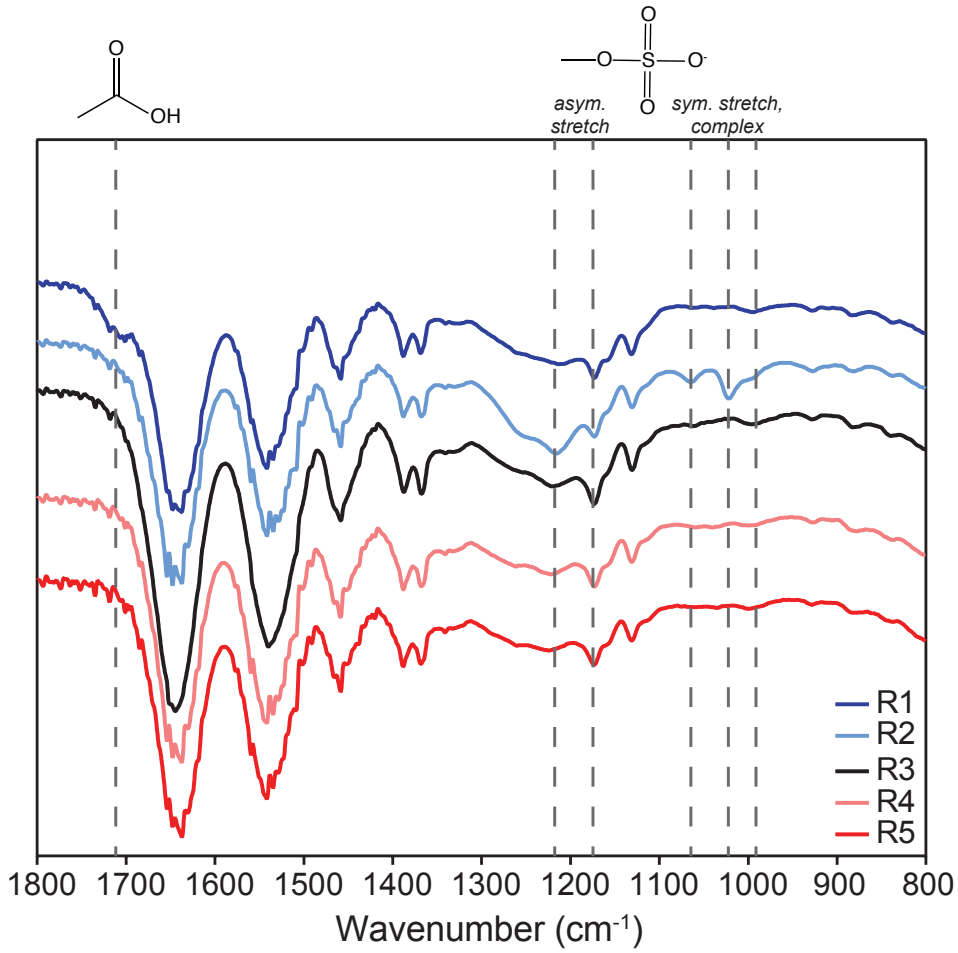

Figure S3. FTIR spectra of modified poly(NIPAM-co-MAA) nanogels. Decrease in the shoulder at 1715 cm^{-1}, corresponding to the carboxyl groups, suggests successful modification. The use of APS as an initiator introduces sulfate groups in the polymer, as evidenced by the bands at 1130 cm^{-1} and 1170 cm^{-1} corresponding to the asymmetric stretching of the sulfur oxygen bonds and the weak band at 990 cm^{-1} corresponding to symmetric stretching. After modification with AEHS (**R2**), additional sulfate bands appeared, specifically at 1020 cm^{-1} and 1060 cm^{-1}, and the intensity of the band at 1210 cm^{-1} increased relative to the band at 1170 cm^{-1}. This is interesting because it has been shown that when sulfates form complexes with metals or protons, the sulfate vibrational bands shift to higher wavenumbers.[1,2] While the sulfate groups from APS are mostly localized on nanogel surfaces, the sulfate-modified carboxyl groups are distributed throughout the nanogel where they can hydrogen bond with the amide bonds of the network. We hypothesize that this complexation resulted in the appearance of S=O bands that are distinct from the pre-existing sulfate bands. For the cationic ligands (i.e., **R3, R4, R5**), modification did not result in distinctive bands in the spectra because of the abundance of N-H and CH_2 bonds already present in the nanogels.

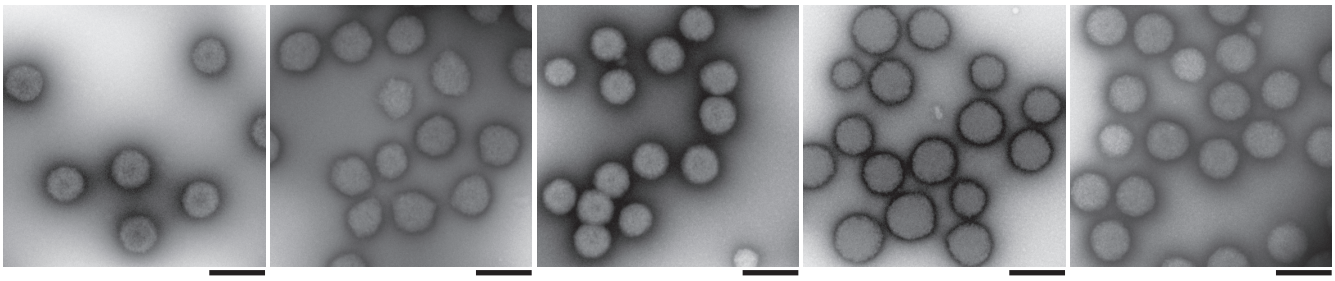

Figure S4. Transmission electron microscopy images of modified poly(NIPAM-co-MAA) nanogels. Nanogels (from left to right: R1, R2, R3, R4, R5) suspended at 0.5 mg/mL in water were probe sonicated, deposited on 400 mesh carbon-coated copper grids, and stained with 2% uranyl acetate. Images were taken at 26,500X magnification. Scale bar represents 300 nm.

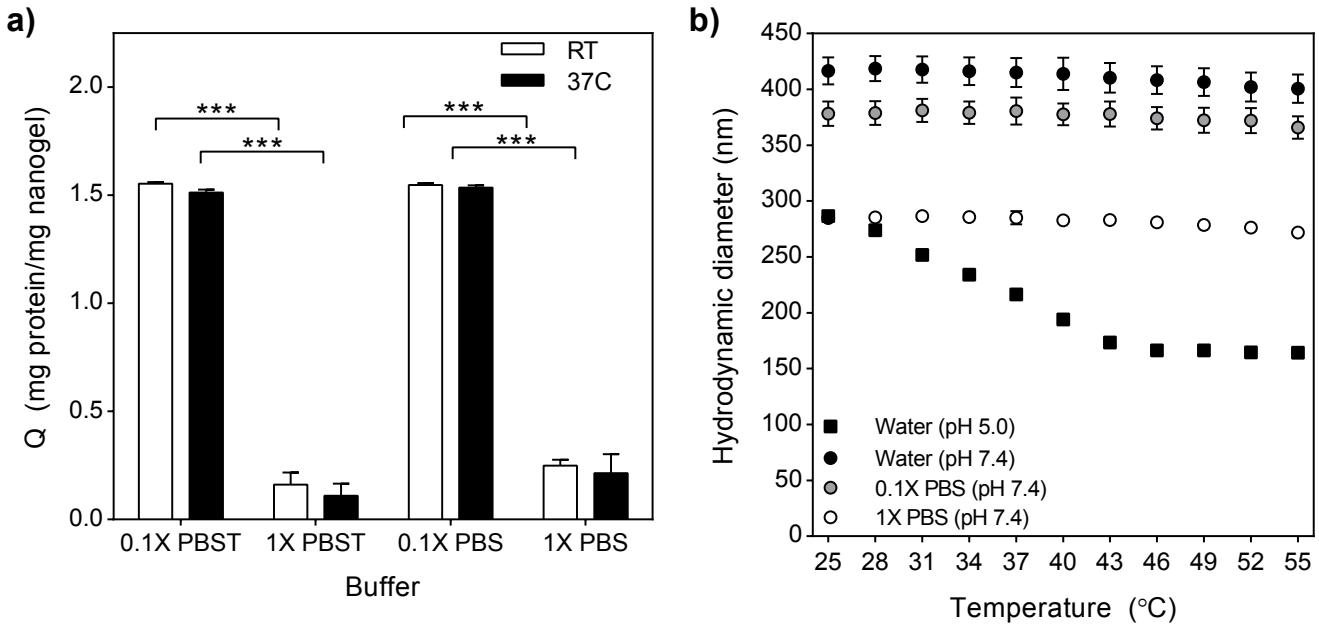

Figure S5. Effects of ionic strength, temperature, and tween 20 on lysozyme binding to R1 nanogels. (a) Increasing ionic strength (0.1X PBS vs. 1X PBS) resulted in a statistically significant decrease in adsorption capacity of **R1** nanogels for lysozyme ($p<0.005$). Increasing the temperature from 25°C to 37°C or including tween 20 (PBS vs. PBST, where PBST = PBS with 0.05% tween 20) did not affect the adsorption capacity of **R1** nanogels for lysozyme. (b) Hydrodynamic diameter as a function of ionic strength and temperature demonstrating that poly(NIPAM-co-MAA) (20 mol% MAA) does not exhibit temperature responsive swelling at pH 7.4.

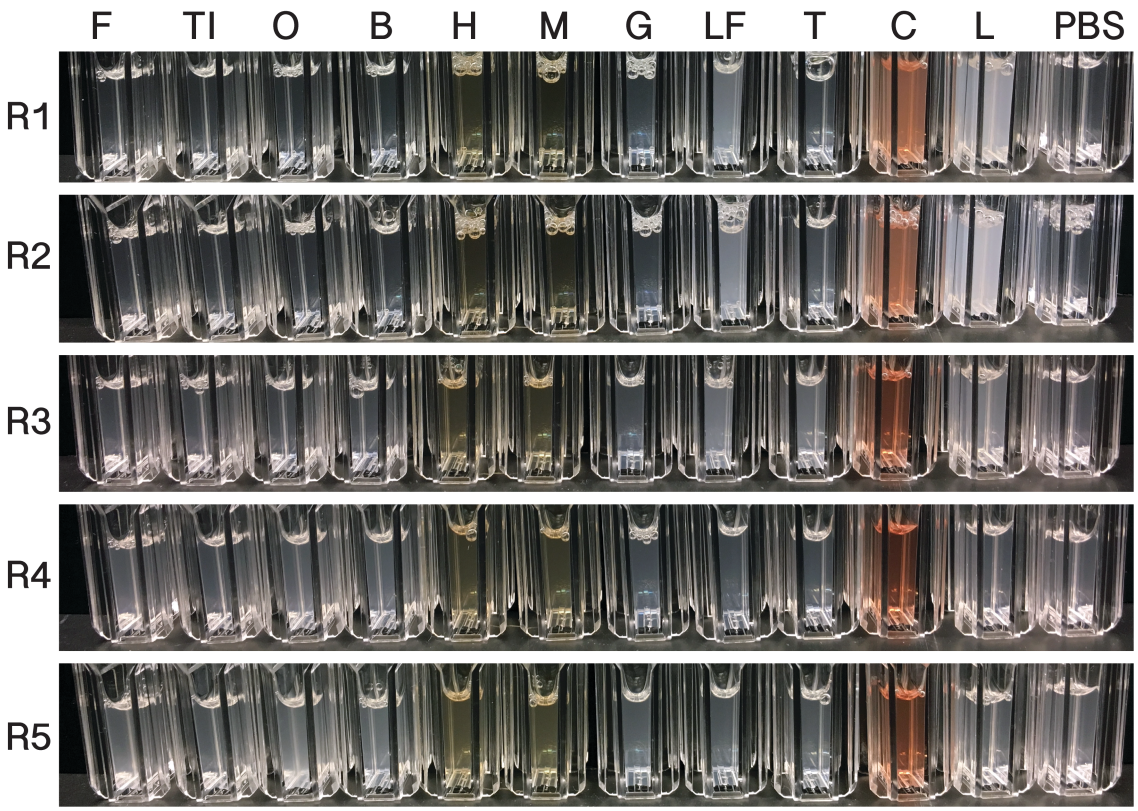

Figure S6. Turbidity changes upon protein binding to charged nanogels in 0.1X PBS (pH 7.4). From left to right: fetuin (F), ovomucoid (aka trypsin inhibitor type II-O) (TI), ovalbumin (O), bovine serum albumin (B), hemoglobin (H), myoglobin (M), gamma globulins (G), lactoferrin (LF), trypsin (T), cytochrome c (C), lysozyme (L), and 0.1X PBS.

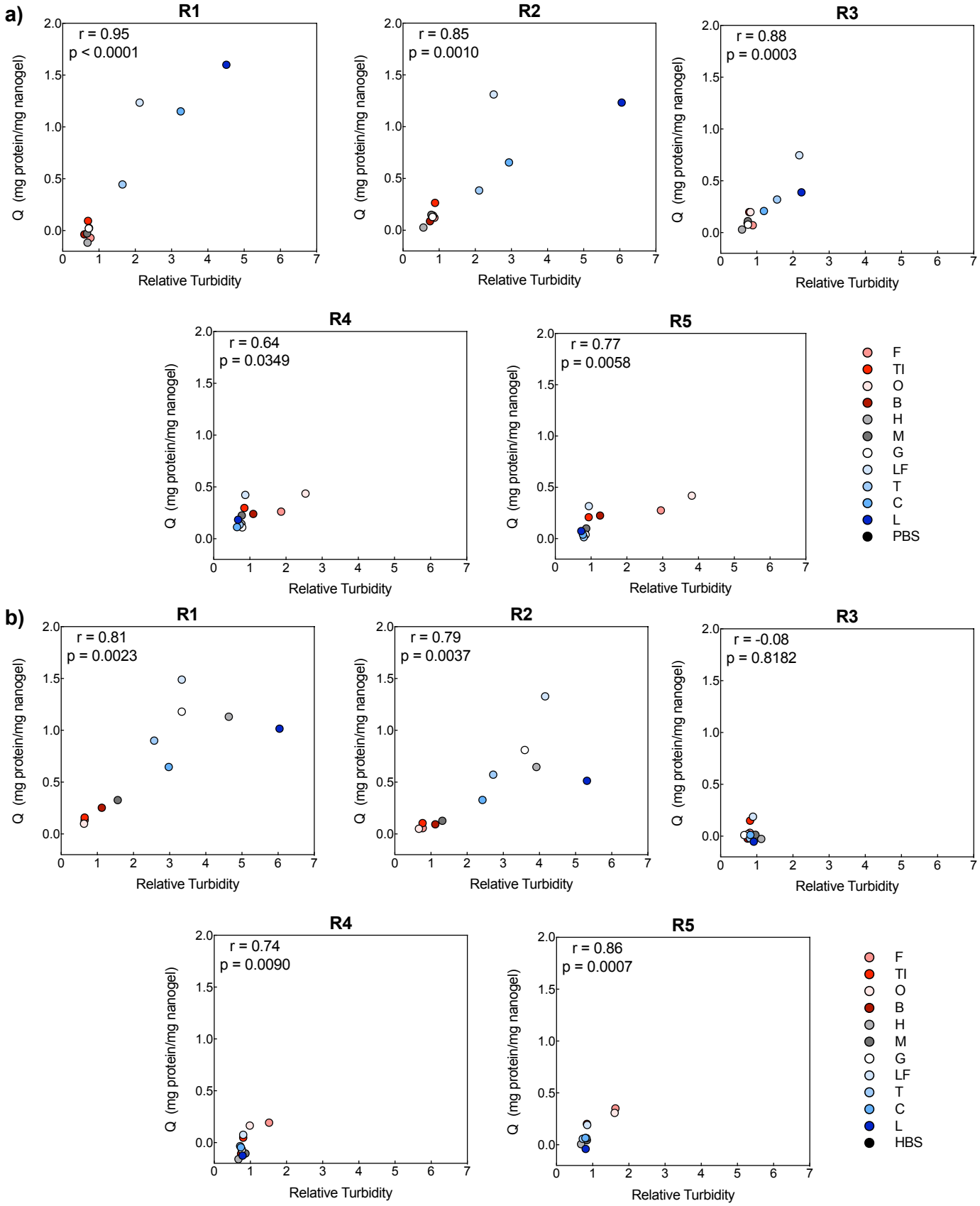

Figure S7. Correlation between relative turbidity and adsorption capacity. Relationship between relative turbidity and adsorption capacity in (a) PBS and (b) HBS. In all cases except for **R3** nanogels in HBS (for which protein binding was undetectable by MicroBCA), there was positive correlation between relative turbidity and adsorption capacity ($r>0$, $p<0.05$).

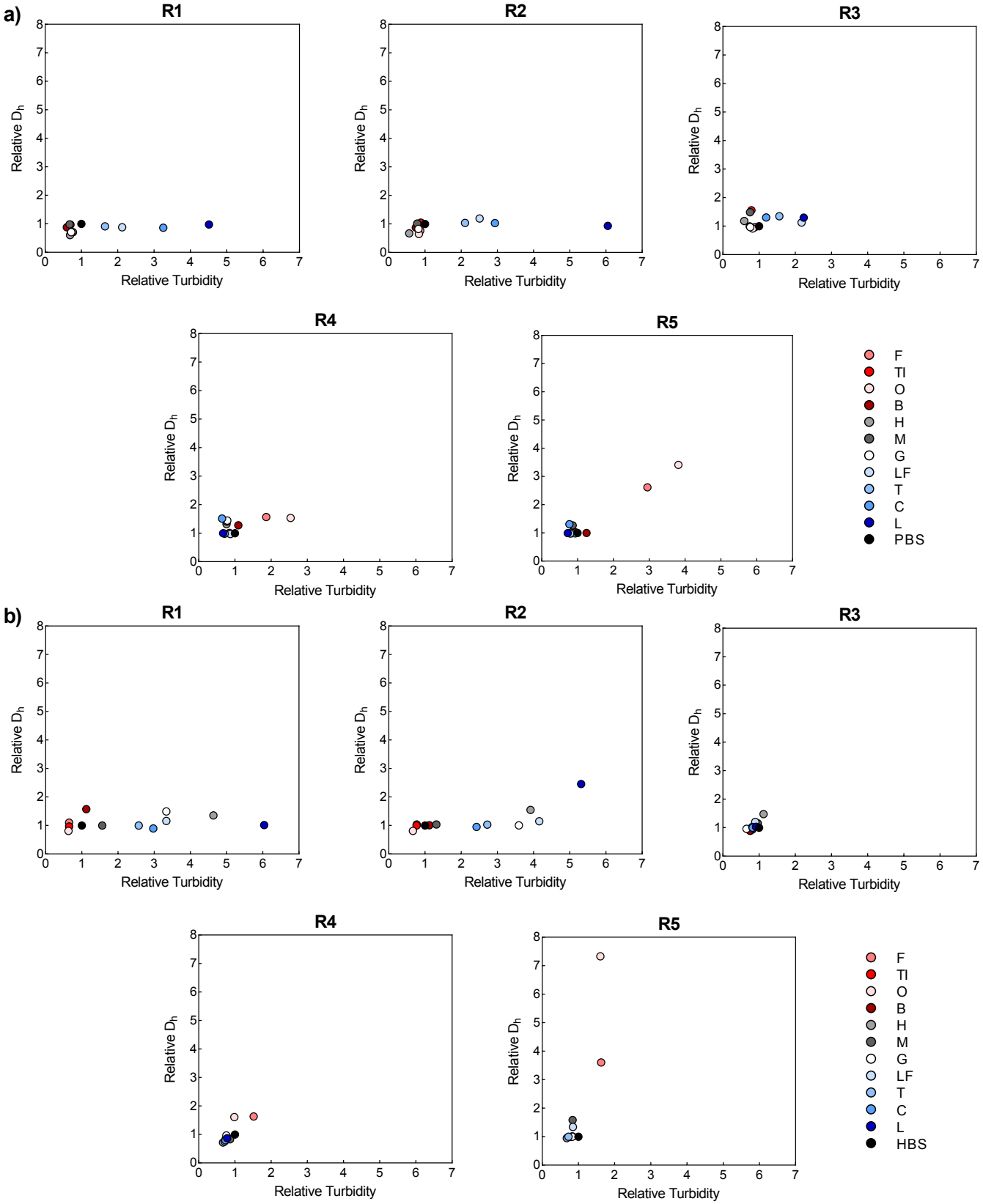

Figure S8. Relationship between relative hydrodynamic diameter (D_h) and relative turbidity. D_h was measured after addition of proteins in (a) 0.1X PBS and (b) 0.1X HBS to determine whether particle aggregation was the reason for increased scattering and, in turn, increased turbidity. For protein-nanogel combinations that did not result in an increase in hydrodynamic diameter (Relative $D_h \sim 1$), the increase in turbidity was attributed to an increase in particle refractive index upon protein binding. Relative D_h was defined as the D_h in the presence of protein divided by D_h in the absence of protein. Relative turbidity was defined as turbidity of the nanogel solution in the presence of protein divided by turbidity in the absence of protein.

Table S1. **Classification accuracy of LDA determined by jack-knife analysis for all receptor combinations.**

	HBS+PBS Classification accuracy (%)	HBS only Classification accuracy (%)	PBS only Classification accuracy (%)
R1 + R2	87.88	81.82	63.64
R1 + R3	87.88	69.70	57.58
R1 + R4	100.00	87.88	78.79
R1 + R5	96.97	63.64	81.82
R2 + R3	87.88	78.79	54.55
R2 + R4	100.00	93.94	81.82
R2 + R5	96.97	78.79	78.79
R3 + R4	96.97	54.55	78.79
R3 + R5	93.94	51.52	72.73
R4 + R5	54.55	45.45	48.48
R1 + R2 + R3	84.85	81.82	57.58
R1 + R2 + R4	100.00	100.00	81.82
R1 + R2 + R5	96.97	84.85	81.82
R1 + R3 + R4	100.00	90.91	78.79
R1 + R3 + R5	96.97	78.79	78.79
R1 + R4 + R5	100.00	84.85	72.73
R2 + R3 + R4	100.00	96.97	78.79
R2 + R3 + R5	96.97	78.79	84.85
R2 + R4 + R5	100.00	96.97	78.79
R3 + R4 + R5	100.00	60.61	78.79
All but R1	100.00	96.97	78.79
All but R2	100.00	93.94	78.79
All but R3	100.00	100.00	78.79
All but R4	100.00	87.88	81.82
All but R5	100.00	100.00	78.79
All	100.00	100.00	81.82

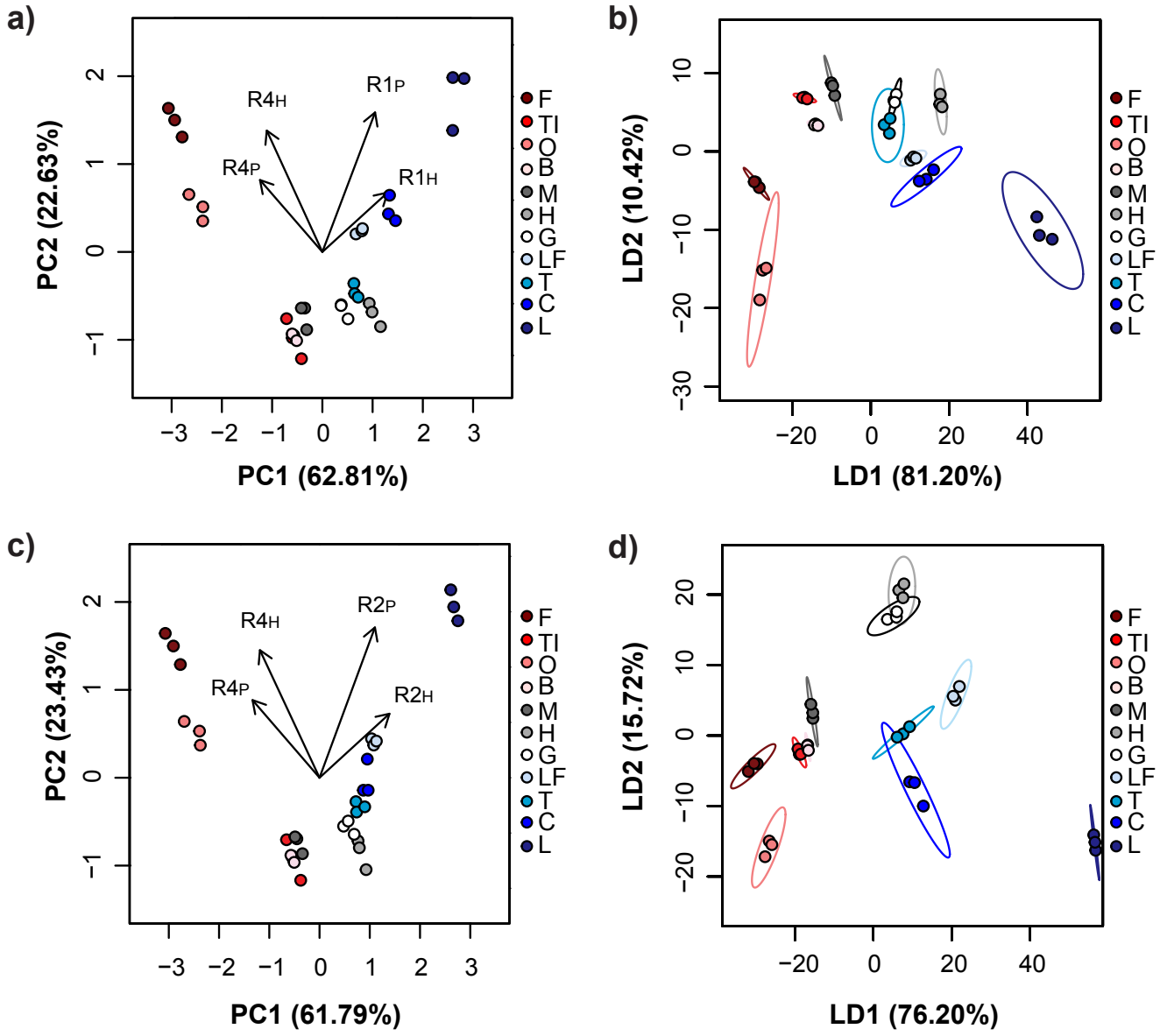

Figure S9. **Multivariate analysis of relative turbidity changes upon protein binding to nanogels**. PCA biplots (a, c) and LDA plots (b, d) correspond to data for protein binding experiments performed with **R1** and **R4** nanogels in both buffers (a, b) or **R2** and **R4** nanogels in both buffers. With both combinations of nanogels, LDA achieved 100% classification accuracy according to jack-knife analysis despite overlap of the confidence ellipses. Red shades = low pI proteins (pI <6.0), gray shades = near-neutral pI proteins (6.0 ≤ pI ≤ 8.0), blue shades = high pI proteins (pI > 8.0). In all cases, protein and nanogel concentrations were 0.5 mg/mL.

Table S2. Components of simulated tear fluid before 1/10 dilution (based on average levels in humans) with 0.1X HBS (pH 5.5).

Component	Concentration (μg/mL)
Mucin (from porcine pituitary)	5
Gamma globulins (from bovine serum)	25
Ovomucoid (tear lipocalin substitute)	175
Lactoferrin (from human milk)	200
Glucose	250
Lysozyme (human, recombinant expressed in rice)	Varied from 0 – 200

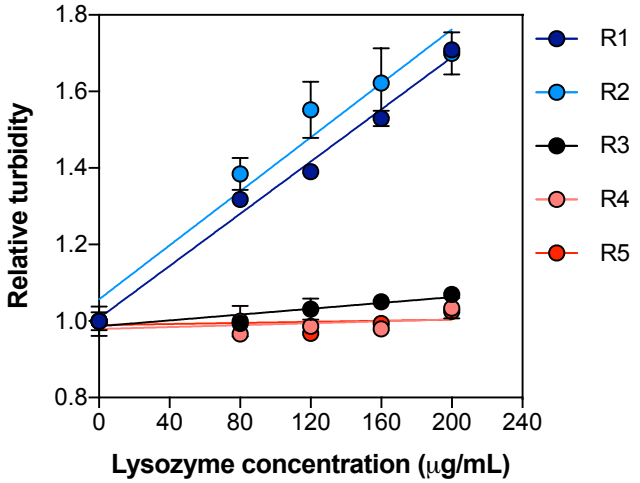

Figure S10. **Turbidity changes as a function of lysozyme concentration in a simulated tear fluid.** Increasing lysozyme concentration in a simulated tear fluid resulted in increased turbidity of nanogel solutions. The sensitivity of the turbidimetric response corresponded to adsorption capacity trends, with R1 and R2 exhibiting the most sensitive changes.

References

1 S. J. Hug, *J. Colloid Interface Sci.*, 1997, **188**, 415–422.
2 D. Peak, R. G. Ford and D. L. Sparks, *J. Colloid Interface Sci.*, 1999, **218**, 289–299.